Crystallinity Vis-à-Vis Two-Phase Models of Oriented Polymers: Inferences from an Experimental Study of Poly(ethylene terephthalate)

VARUNESH SHARMA,[1] PRASHANT DESAI,[1] A. S. ABHIRAMAN[2]

[1] School of Textile and Fiber Engineering, Polymer Education and Research Center, Georgia Institute of Technology, Atlanta, Georgia 30332

[2] School of Chemical Engineering, Polymer Education and Research Center, Georgia Institute of Technology, Atlanta, Georgia 30332

Received 24 December 1996; accepted 24 January 1997

ABSTRACT: Extensive measurements with poly(ethylene terephthalate) fibers of a broad range of orientational and crystalline order have been made and analyzed vis-à-vis two-phase (crystalline and noncrystalline) descriptions of solid polymer morphologies. The results show that no two fundamentally different methods provide the same estimates, or consistently even the same trends, of phase composition over a broad range of order. Modifications of the simple two-phase model by incorporating order-dependence of characteristic parameters, such as noncrystalline density, still lead to unsatisfactory results. No meaningful relationship has been found between such parameters and measures of order, such as calculated birefringence and *trans* content of the noncrystalline phase. However, because of the simplicity of two-phase models and the absence of any objective framework for correlating properties with measures of order with three or more phase compositions, continued use of two-phase models, with cognizance of their inherent limitations, is recommended in seeking directions for process and product development. © 1997 John Wiley & Sons, Inc. J Appl Polym Sci **65:** 2603–2612, 1997

Key words: poly(ethylene terephthalate); crystallinity; two-phase morphology

INTRODUCTION

The extent of crystallization (crystallinity) in crystallizable oriented polymers is estimated using various techniques including X-ray scattering, calorimetric analysis, density measurement, vibrational spectroscopy, and polarized optical microscopy. Even though the principles behind these techniques are well understood, their application in the determination of crystallinity in polymers is not free of ambiguities. The crystalline phase in semicrystalline polymers is frequently estimated using a two-phase model. Prominent among the two-phase morphological models are (1) crystal lamellae alternating with amorphous layers, (2) the fringed micelle model in which segments of polymer chains align to form crystals but also pass through the amorphous regions, and (3) spherulitic structures.[1] Ideally, the two phases are perfect crystals and ideal supercooled melt (amorphous phase).[2] Crystallinity is usually calculated assuming invariant structures (with respect to the technique being used) *within* each of the two phases. Also, when the information obtained from one technique is utilized by another for the determination of crystallinity, it is invariably assumed

Correspondence to: A. S. Abhiraman.

Journal of Applied Polymer Science, Vol. 65, 2603–2612 (1997)
© 1997 John Wiley & Sons, Inc. CCC 0021-8995/97/132603-10

that they distinguish the two phases in the same manner. However, it has been seen that different techniques of determining crystallinity do not necessarily yield the same values for a given polymer specimen.[3–5]

Studies related to individual techniques, comparison of different methods for estimating crystallinity, and multiphase (more than two phases) models have been reported.[3–11] For example, it has been concluded that it is not possible to determine crystallinity by infrared (IR) technique alone because true crystalline bands do not exist in most polymers.[4] Nuclear magnetic resonance (NMR) and X-ray techniques have been successful in looking at possibilities other than those of just the two phases.[6–11] On the basis of NMR measurements on polyethylene fibers, Hyndman and Origlio have described a three-phase model. They observed a proton absorption line intermediate in width between that of the crystal phase and that of the amorphous phase. They describe the structure in terms of crystalline, oriented amorphous, and amorphous phases.[6] In X-ray studies of polyethylene, polystyrene, and nylon-6, Murthy et al. characterized amorphous orientation by separating the amorphous scattering into oriented and unoriented components.[8] Fu et al. have been able to obtain a two-dimensional, noncrystalline, wide-angle X-ray scattering pattern for poly(ethylene terephthalate) (PET) fibers.[9] The anisotropic noncrystalline scattering intensity was attributed to liquid-like amorphous scattering and that of an oriented intermediate phase. This oriented intermediate phase represents mainly "the material between the crystals across the PET fiber." In NMR studies of PET fibers and films, English observed a less mobile amorphous phase in relaxation experiments,[10] suggesting a three-phase model. His semiquantitative model of chain motion in PET requires the existence of three different environments in these phases. English also observed dipolar line shapes arising from crystalline, amorphous regions, and a broad component from less mobile amorphous regions. Tzou et al. studied the morphology and orientational order of PET fibers using solid-state NMR techniques.[11] To describe morphology in PET fibers, they needed a model consisting of at least four different *microenvironments,* that is, (1) crystalline, (2) noncrystalline with order in both carbonyl and glycoethylene environments, (3) noncrystalline with order only in glycoethylene environment, and (4) amorphous.

In spite of all of the above-mentioned studies that suggest the need for more than two phases to describe oriented semicrystalline polymers, the two-phase model remains the most frequently used to estimate crystallinity. Wide usage and acceptance of the two-phase model is based on its simplicity and capability, real or perceived, to provide correlations with mechanical properties. It is, therefore, necessary to determine and, if possible, rationalize the differences and agreements that might exist in crystallinities determined through different techniques within the context of two-phase models.

In order to carry out effectively a comparison of crystallinities obtained via different techniques, a comprehensive experimental study has been conducted with PET of a broad range of orientational and crystalline order. An attempt has also been made to obtain quantitative information regarding order in the noncrystalline phase of oriented PET, again within the context of a two-phase model. The experimental techniques used are calorimetric analysis, bulk density measurements, X-ray scattering, Fourier transform infrared (FTIR) spectroscopy, and interference microscopy. PET samples with a broad range of crystalline and orientational order were generated using a combination of different melt extrusion and drawing conditions. Since the glass transition temperature of PET is significantly above room temperature, it allowed storage with "frozen in" levels of orientation and crystallinity during the course of this study.

EXPERIMENTAL DETAILS

Materials

The experimental PET fibers (Table I) were specifically produced for this study under the following conditions in an industrial pilot plant facility. The fibers were melt spun at 298°C over a range of spinning speeds, low (2,000 m/min, sample A), intermediate (3,000 and 4,000 m/min, samples B and C, respectively), and high (4,500, 5,000, and 5,500 m/min, samples D, E, and F, respectively). The intrinsic viscosity, measured at 25°C in a 60 : 40 (v : v) phenol-tetrachloroethane mixture, was 0.65 dL/g. The finish on the as-spun fiber was $\sim$ 1.2% by weight. The drawn sample (J), obtained from industry, was spun at 1,800 m/min and stretched to a draw ratio (DR) of 2.7. Samples G and H were produced by drawing sample B at

Table I Specifications of the PET Fibers Used

Fiber	Sample Code	Spinning Speed (m/min)	Linear Density (denier)	DR	Oven Temperature (°C)	Godet Temperature (°C)
As spun	A	2,000	97			
	B	3,000	97			
	C	4,000	97			
	D	4,500	97			
	E	5,000	98			
	F	5,500	97			
Drawn	G	3,000	49	1.9	75	
	H	3,000	40	2.4	150	
	J	1,800	70	2.7	Commercial grade	
	K	Industrial	997			
	L	Industrial	977	1.05	150	240
	M	4,500	100	1.9	150	240

two different temperatures, 75 and 150°C, respectively.

A commercially available industrial PET fiber (sample K) was also used in this study. No sample information was available from the manufacturer. This industrial PET fiber was also further drawn to a DR of 1.05, with the draw roll temperature at 150°C and the oven temperature at 240°C (sample L). One of the drawn samples (sample M) included in this study was originally used by other researchers at Georgia Institute of Technology.[12] The spinning speed for this sample was 4,500 m/min. It was drawn with DR = 1.9 under the same conditions as for sample L.

Methods for Determination of Crystallinity

Calorimetric Analysis

A Seiko DSC-220 was used for calorimetric analysis of a small quantity (approximately 5 mg) of finely chopped fibers (length less than 2 mm). A standard indium sample was used to calibrate DSC-220. Three specimens of each sample were analyzed. Small holes were made in the aluminum lid to allow a dynamic nitrogen gas environment over the fibers in the aluminum pan. Each measurement consisted of heating from 30 to 300°C at a rate of 10°C/min. Crystallinity was calculated, assuming the enthalpy of melting of crystals, ΔH_m^*, to be 138 J/g[13]. The crystalline mass fraction is then given by

$$X_{c,m} = \frac{\Delta H_{m,x}}{\Delta H_m^*} \qquad (1)$$

where $\Delta H_{m,x}$ is the enthalpy of the melting of the sample. If any detectable crystallization occurred during the heating of the sample to its melt ("cold crystallization"), $\Delta H_{m,x}$ was obtained by subtracting the enthalpy of cold crystallization from the measured enthalpy of melting. The usual assumption here is that the standard enthalpies of crystallization and melting are the same. A significant error can occur in this regard as a result of crystallization from different levels of precursor orientation. Higher orientation in the precursor would mean a higher *trans*-to-gauche ratio and thus a lower internal energy of the precursor. Consequently, the enthalpy per unit mass of cold crystallization would also be lower, leading to an overestimation of the enthalpy of the melting of the crystals in the precursor.

Optical Density and Birefringence

With plane-polarized light, the refractive indices parallel, $n_{\|}$, and perpendicular, $n_{\perp}$, to the fiber axis were measured on an Aus Jena Interphako interference microscope. For fibers possessing axial symmetry, isotropic polarizability, β_{iso}, is given by

$$\beta_{iso} = \frac{\beta_{\|} + 2\beta_{\perp}}{3} \qquad (2)$$

where $\beta_{\|}$ and $\beta_{\perp}$ are, respectively, the polarizations parallel and perpendicular to the symmetry axis. If the birefringence, $\Delta n = n_{\|} - n_{\perp}$, is much less than the two refractive indices, the corre-

sponding isotropic refractive index can be approximated by

$$n_{iso} = \frac{n_{\parallel} + 2n_{\perp}}{3} \tag{3}$$

The Lorentz–Lorenz equation can be used to relate the isotropic refractive index of a material to its density[14] as

$$\left(\frac{n_{iso}^2 - 1}{n_{iso}^2 + 2}\right) = \chi\rho_L \tag{4}$$

where χ is the specific refractivity, and ρ_L is the Lorentz (optical) density. This relation for PET has been determined to be[14]

$$\rho_L = 4.0486\left(\frac{n_{iso}^2 - 1}{n_{iso}^2 + 2}\right) \tag{5}$$

This approximation is valid for PET, provided the birefringence is less than 0.1.[14] The birefringence and optical density were calculated from the averages of 10 measurements on filaments of a specimen. Amorphous birefringence (Δn_a) was also calculated using X-ray crystallinity values, assuming a two-phase model with the "form birefringence" being negligible, using the simple mixture rule as follows:

$$\Delta n = \Delta n_a(1 - X_{c,m}) + \Delta n_c^* f_c X_{c,m} \tag{6}$$

where Δn_c^* (=0.22)[15] is the intrinsic crystalline birefringence of PET, and f_c is the Hermans' crystallite orientation function.

The optical method provides, in addition to density, information regarding uniformity of structure through the uniformity of fringes across the observed cross section. All of the fibers used in this study exhibited radial uniformity in structure.

Bulk Density

Mass extent of crystallization, $X_{c,m}$, was calculated with bulk densities measured by two techniques, density gradient column and helium pycnometry:

$$X_{c,m} = \left(\frac{\rho_c}{\rho}\right)\left(\frac{\rho - \rho_a}{\rho_c - \rho_a}\right) \tag{7}$$

where ρ, ρ_a, and ρ_c are, respectively, the densities of the sample, ideal amorphous phase, and perfect crystals.

The density gradient column was prepared using higher (ρ = 1.5 g/cm^3) and lower (ρ = 1.28 g/cm^3) density solutions of calcium nitrate in water. The density range of the column was selected to cover the completely amorphous to the crystalline range (ρ_a = 1.335 g/cm^3 to ρ_c = 1.529 g/cm^3 [16]) of the PET fiber samples. The whole column with a linear density gradient was maintained at a constant temperature (23°C) using a water jacket around it. The fibers were wetted out with the lower density solution before they were introduced in the column. The final reading of the fiber's location in the column, obtained 24 h after the introduction of the fibers, was used with the calibration plot for the column to determine the density of the samples. Three specimens of each fiber sample were used for measurement.

A Quantachrome® Helium Pycnometer (model MVP-1) was used to measure the volume of a known mass of PET fibers. Approximately 5 g (accurately weighed) of a PET sample was packed in the sample sleeve of the helium pycnometer and enclosed in the sample cell. It was purged for 30 min to remove air and moisture before the measurement was made. After the sample cell was purged, the reference cell (fixed and known volume) was pressurized with helium to about 17 psi. Then, the gas was allowed to occupy both the reference and the sample cells and the final pressure reading was noted. The pressure difference between the final and initial states is used to calculate the volume of the sample (V_P), assuming helium behaves like an ideal gas,[17] as

$$V_P = V_C - V_R\left(\frac{P_1}{P_2} - 1\right) \tag{8}$$

where V_C is the cell volume, V_R is the reference volume, and P_1 and P_2 are the pressure above the ambient in the reference cell and the final lower pressure in the sample cell, respectively. Measurements were made on three specimens of each fiber.

Wide-Angle X-Ray Scattering

A Rigaku-Rotaflex θ-2θ diffractometer with rotating copper anode, operating at 100 mA and 45 kV, was used to obtain radial, equatorial, meridional, and azimuthal scans. A standard nickel filter was

used for attenuating the K_β component in the incident beam. The radial scans were used to calculate percent crystallinity using Ruland's method.[18] This method is preferred over the other methods because it does not require any amorphous or crystalline standards. A flat layer of parallel yarns was wound on a sample holder that was rotated at 60 rpm around an axis perpendicular to the sample plane during the radial scans over the angular range of 5 to 75° 2θ. Data collection times were selected to ensure multiple complete revolutions of the sample holder. Corrections for air scattering, Lorentz-polarization factor, and absorption were made using the crystallinity analysis software from Rigaku. A linear absorption coefficient of 9.416/cm of sample thickness was used to make absorption corrections. Crystallinity was obtained as the ratio of integrated intensities of the corrected crystalline and the corrected total scattering. Two tasks were difficult to perform with samples of relatively low crystallinity: (1) separation of intensity contributions from the two phases, and (2) estimation of the width of crystalline diffraction peaks. Ruland's method could not be applied to the least crystalline sample (sample A), which produced only an amorphous scattering and was considered to be noncrystalline for this study.

Hermans' crystalline orientation function, f_c, was estimated from the azimuthal intensity distribution, $I(\phi)$, of the $(\bar{1}05)$ peak as

$$f_c \approx f_{\bar{1}05} = \tfrac{1}{2}(3\langle \cos^2\phi_{\bar{1}05}\rangle - 1) \qquad (9)$$

where

$$\langle \cos^2\phi\rangle = \frac{\int_0^{\pi/2} I(\phi)\sin\phi\,\cos^2\phi\,d\phi}{\int_0^{\pi/2} I(\phi)\sin\phi\,d\phi} \qquad (10)$$

FTIR Spectroscopy

FTIR spectra of PET fibers were obtained using a Bio-Rad Instrument FTS-60A with a Labsphere integrating sphere, a KBr beam-splitter, an MCT detector, and a ceramic source. A gold coin (1.5-inch diameter) with 95% reflectivity in the mid-IR region (4,000–400 cm^{-1}) was placed behind the sample bundle of fibers weighing $\sim$ 5 g. The sample chamber was purged with dry air for $\sim$ 1 h to remove moisture. The spectra were obtained in the reflection mode at a resolution of 8 cm^{-1} over the range of 700–4000 cm^{-1}, with 256 scans averaged for each sample. IR spectrum of PET film (Mylar) taken in the transmission mode was compared with spectra taken in the reflection mode with the integration sphere to ensure that no additional features were introduced in the spectra because of the integrating sphere. Integrating sphere optics were used to minimize problems in analysis due to multiple scattering.

The *trans* content was calculated using IR bands corresponding to —C—O— stretch mode in *trans* (973 cm^{-1}) and gauche (1042 cm^{-1}) conformations of glycoethylene moiety[19] as

$$\%Trans = \frac{A_{973}}{A_{973} + A_{1,042}} \times 100 \qquad (11)$$

The *trans* content of the amorphous phase ($\%T_a$) was estimated, assuming no gauche in the crystalline phase and a simple additivity of the *trans* contribution from the two phases to the spectrum, as follows:

$$\%T_a = \frac{\%Trans - \%X_{c,m}(\text{X-ray})}{100 - \%X_{c,m}(\text{X-ray})} \times 100 \qquad (12)$$

RESULTS AND DISCUSSION

The crystallinities obtained from different techniques, assuming a two-phase model with invariant characteristic parameters for each phase, are shown in Figures 1(a–e). It is clear from these and the summary plot (Fig. 2) that considerable differences exist in the estimates of simple two-phase crystallinity by the different methods. These differences extend beyond a lack of just quantitative correspondence, that is, *no two methods even provide consistently the same trend* in their estimates of crystallinity. It is therefore important to recognize that significant errors can arise in any attempt to predict properties of oriented polymers which might require input from two or more of these techniques, especially if such predictions are based on two-phase (crystalline and noncrystalline) models with invariant characteristic parameters assumed for each phase.

The data presented in Figure 1 have been explored in detail to determine if

- useful inferences can be made from any combination of measures vis-à-vis order in bulk polymers, and

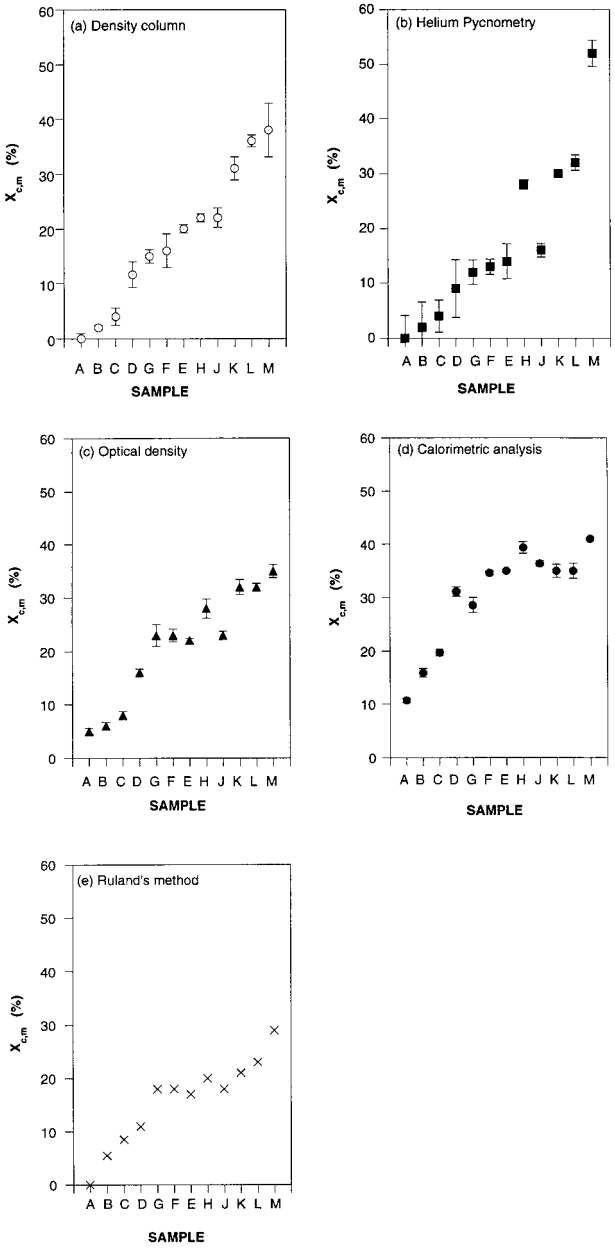

Figure 1 Crystallinity values of PET samples calculated using different techniques: (a) bulk density from density gradient column, (b) bulk density from helium pycnometry, (c) optical density from isotropic refractive index, (d) from differential scanning calorimetry analysis, (e) wide-angle X-ray diffraction (Ruland's method).

- the data can be rationalized within the context of a two-phase model, but with the noncrystalline phase's characteristics being dictated by some measure of order that might exist in it.

Density and Order in the Noncrystalline Phase

A common inference regarding differences between crystallinities obtained via bulk density and wide-angle X-ray scattering is that it is possibly a reflection of changes in the density of the noncrystalline phase due to its orientation.[20] In order to explore this aspect, the noncrystalline density, ρ_a, of each sample was estimated accepting the crystallinity, $X_{c,m}$, *obtained from the X-ray method,* and bulk density, ρ, using eq. (7), i.e.,

$$\rho_a = \frac{\rho\rho_c(1 - X_{c,m})}{(\rho_c - \rho X_{c,m})} \tag{13}$$

Birefringence of the noncrystalline phase, Δn_a, of each sample was computed with eq. (6), using the crystalline orientation function, f_c, and the mass fraction crystallinity, $X_{c,m}$, obtained from the X-ray method. The estimated noncrystalline density is plotted against the birefringence of this phase in Figure 3(a–c). The three figures correspond to ρ_a estimates from the gradient column, helium pycnometry, and optical density. The lack of correlation suggests that a modification of the two-phase model with invariant crystalline phase parameters and orientation-dependent noncrystalline density is not sufficient. Even if the analysis is restricted to samples from the same process, such as, for example, melt spinning at different

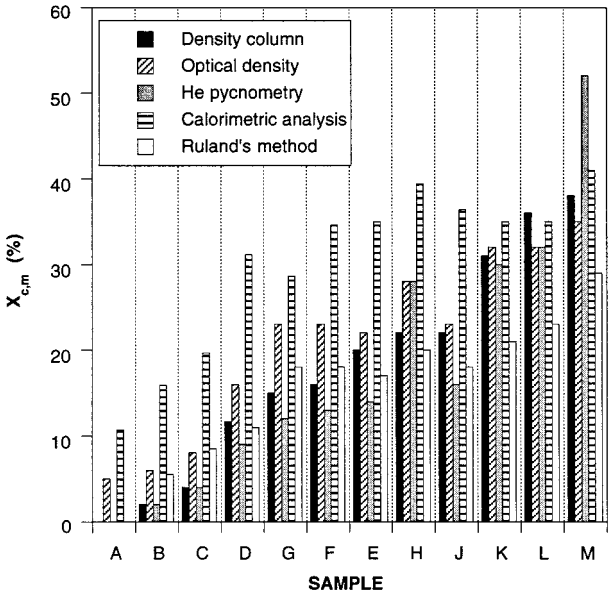

Figure 2 Comparison of crystallinity values of PET samples obtained by different techniques.

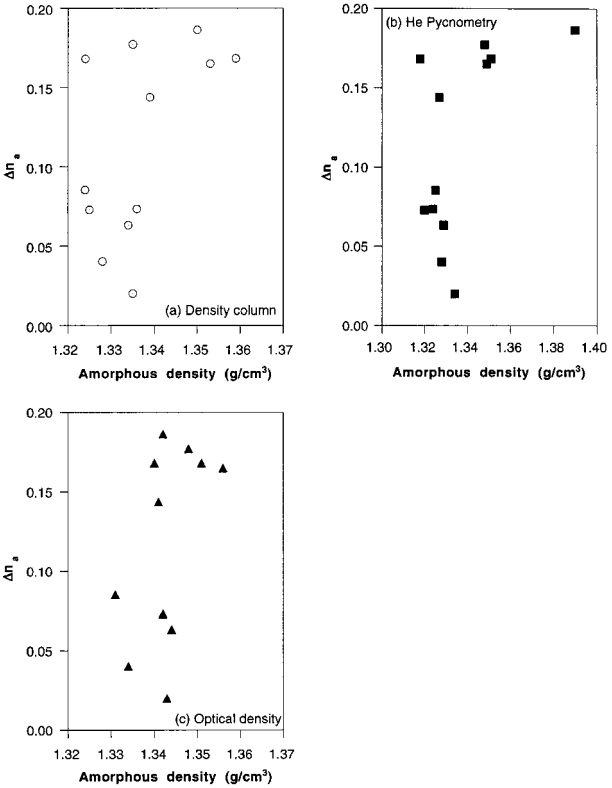

Figure 3 Amorphous birefringence in PET samples versus amorphous density calculated from the density measured by (a) density gradient column, (b) helium pycnometry, (c) isotropic refractive index (measured by interference microscopy).

speeds with no additional processing, there is still a lack of correlation between the estimated noncrystalline phase density and its birefringence.

Orientation and *trans* Content of the Noncrystalline Phase

The *trans* content of the ethylene glycol residue of PET, obtained from the *trans* and gauche IR bands corresponding to —C—O— stretch, CH_2 wag, and CH_2 rock, are shown in Figure 4 as a function of the measured bulk density of the material. For reasons that are not clear, the estimates from the three modes fail to exhibit even similar trends. Also, there is no correlation between the *trans* content and the bulk density. Previous workers in this area have investigated correlations between the total *trans* content and bulk density.[20] Proposing such correlations, however, would imply erroneously that the densities of the *trans* environment in the different phases are the same. The birefringence and density of the noncrystalline phase (computed using density values from the density gradient column) are shown in Figure 5 against the conformational composition of the noncrystalline phase, computed by assuming that the *trans* fraction of the material in the crystalline phase corresponds to that of the crystalline fraction obtained via X-ray scattering. It is clear that even in these uniaxially oriented materials, there is no correlation between these measures.

Calorimetry and Conformational Composition of the Noncrystalline Phase

An obvious feature in the data of Figures 2 and 6 is that, when crystallization occurs during thermal analysis, that is, when the temperature is raised above the glass transition temperature of PET, a higher crystallinity is estimated by calorimetric analysis than any of the other methods. Even when no directly detectable crystallization occurs during the analysis, the crystallinity from calorimetry is generally higher than the values yielded by the other methods. The reason for this difference appears to be in the conformational composition of the noncrystalline phase, which can influence the enthalpy of cold crystallization

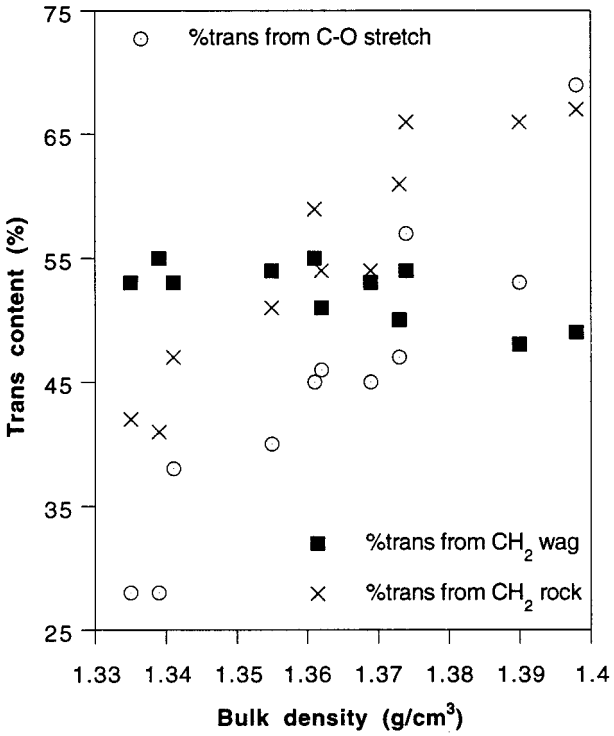

Figure 4 *trans* content in PET samples versus bulk density from density gradient column.

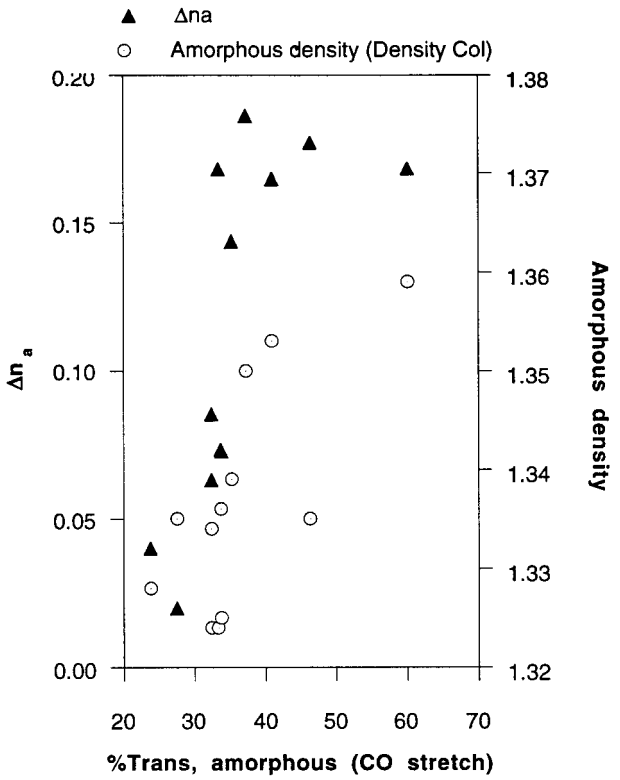

Figure 5 Calculated amorphous birefringence and amorphous density in PET samples versus amorphous *trans* content calculated from the C—O stretch band.

as well as melting. This influence on the estimation of crystallinity in the initial material is discussed below.

Conformation and Cold Crystallization

The two preferred conformations in PET are *trans* and gauche. It is known that only the *trans* conformation of the ethylene glycol residue exists in the crystalline phase in PET, whereas a distribution of rotational isomers exists in the noncrystalline phase.[21] It is reasonable to expect preferred transformation of noncrystalline *trans* sequences to the crystalline phase during crystallization, especially if crystallization occurs in an oriented precursor. The gauche conformation is relatively higher in energy than the *trans* conformation, the difference between them being ~ 1.65 kcal/mol of PET.[22] Therefore, if cold crystallization occurs before melting in calorimetric analysis, the transformation of the noncrystalline phase to the crystalline phase could involve a relatively lower fraction of the gauche conformations changing to the *trans* conformations and thus lead to an underestimation of enthalpy of cold crystallization. Subtraction of this enthalpy from the total enthalpy of melting, for the *determination of enthalpy of melting of preexisting crystals,* can thus lead to overestimation of crystallinity by as much as 25%. Conformational composition of the noncrystalline phase can also have an effect of similar magnitude on the enthalpy of melting if this composition is different from that of the melted polymer. It can lead to overestimation or underestimation, depending on whether the noncrystalline phase has been constrained by the morphology to have a *trans* content that is more or less than that of the constraint-free melt.

CONCLUSION

Results from the extensive measurements with PET fibers of a broad range of orientational and crystalline order point clearly to the following vis-à-vis two-phase (crystalline and noncrystalline) descriptions of solid polymer morphologies.

- No two fundamentally different methods pro-

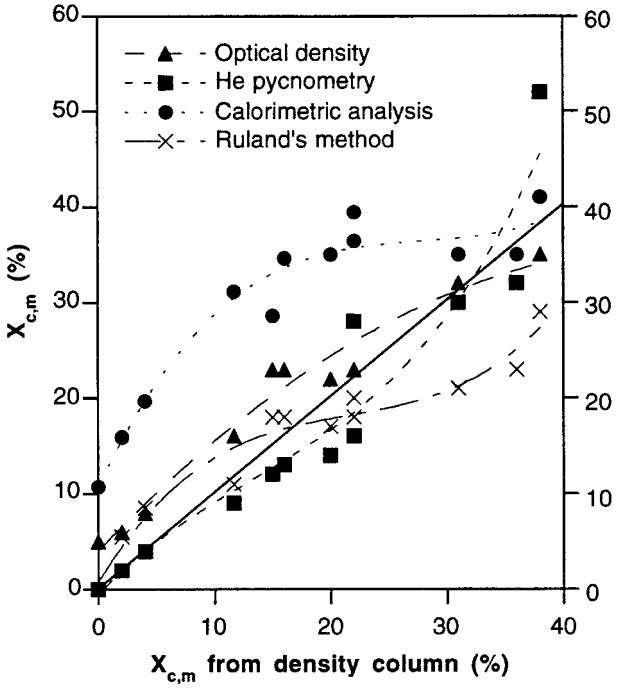

Figure 6 Comparison of crystallinity values in PET samples with the crystallinity values obtained using density gradient column. The solid line represents a one-to-one correspondence between the crystallinity values.

Table II Differential Scanning Calorimetry of PET Yarns

Sample	ΔH_c (mJ/mg) (1st Heating)	ΔH_m (mJ/mg) (1st Heating)	$\Delta H_{m,x}$ (mJ/mg) (1st Heating)	$X_{c,m}$ (%)= $\frac{\Delta H_{m,x}}{\Delta H_m^*} \times 100$
A	−25.8	40.5	14.7	11
B	−20.4	42.3	21.9	16
C	−17.7	45.0	27.2	20
D	−7.4	50.2	42.9	31
E	−2.7	51.0	48.4	35
F	−2.5	50.3	47.8	35
G	−11.8	51.3	39.5	29
H	0.0	54.4	54.4	39
J	0.0	50.2	50.2	36
K	0.0	48.2	48.2	35
L	0.0	48.4	48.4	35
M	0.0	56.6	56.6	41

ΔH_m^* = 138 mJ/mg. $\Delta H_{m,x} = \Delta H_m + \Delta H_c$.

vide the same estimates of phase composition over a broad range of order in the same polymer.

- Modifications of the simple two-phase model by incorporating order-dependence of characteristic parameters, such as noncrystalline density, also lead to unsatisfactory results. No meaningful relationship has been found between such parameters and measures of order, such as calculated birefringence and *trans* content, of the noncrystalline phase.
- If calculations are performed assuming invariant phase characteristics, the procedures for obtaining a measure of any order within the noncrystalline phase would lack general validity because they would invariably involve coupling of data from two or more methods that provide different estimates for the phase composition.

Table III *trans* Content and Amorphous Birefringence of PET Yarns

Sample	% *Trans*	% T_a [a]	Δn_a
A	28	28	0.020
B	28	24	0.040
C	38	32	0.085
D	40	32	0.063
E	45	34	0.073
F	46	34	0.073
G	45	33	0.168
H	57	46	0.177
J	47	35	0.144
K	53	41	0.165
L	69	60	0.168
M	55	37	0.186

[a] T_a, *trans* content in the amorphous phase.

In spite of these deficiencies, two-phase models have been, and continue to be, widely used in seeking process-structure-property relations in bulk polymers. The primary reasons for continued predominance of two-phase models are

- It is relatively easy to make the required measurements.
- They are amenable to analysis through relatively simple thermodynamic and kinetic models of the formation of one of the phases from the other.
- They do yield useful correlations, provided the data are limited to materials from a given process, with essentially the same morphology.
- The results are amenable to relatively straightforward interpretations.

These advantages have led to a large number of published and unpublished reports of correlations, such as "amorphous" orientation versus strength, "amorphous" orientation versus shrinkage above T_g, and so forth. While there is a preponderance of such evidence, it should be noted that each of these reports pertains, individually, to a narrow context and that no general correla-

tion has been found for a material fabricated by different processes and over a broad range of processing conditions.

Recognition of the deficiencies in two-phase models has led to several studies aimed at quantitative separation into three or more phases as well as introduction of new methods for "phase" decomposition/separation. Examples of these are the three-phase models of Wunderlich et al.,[9] with crystalline, amorphous, and oriented intermediate phases that are decomposed via removal of the crystalline contribution from the total diffraction pattern, and Murthy with crystalline, oriented amorphous and isotropic amorphous phases determined via X-ray scattering,[8] as well as the four-phase model of Tzou et al. for PET[11] determined through a combination of solid-state NMR and density measurements. There is clear evidence in each case to justify the resolution of phase composition into more than two phases. There is also ample justification for other criteria, such as mobility as determined by solid-state NMR[23,24] and dynamic mechanical analysis,[25] in the methods for phase decomposition.

It is necessary to develop at least two fundamental links before these complex phase decompositions can become useful in establishing process–structure–property relations: (1) a framework for thermodynamic and kinetic models for the formation of the different phases, including evolution of distribution of order, if any, within any of the phases; (2) a framework for quantitatively relating the phase sizes and concentrations, phase structures, and morphology to the relevant physical properties. Until there is sufficient progress in this regard, continued use of two-phase models, with cognizance of their inherent limitations, is recommended in seeking directions for process and product development.

The authors gratefully acknowledge partial funding of this research through a grant from the NASA-HiPPAC Center.

REFERENCES

1. F. W. Billmeyer, *Textbook of Polymer Science,* Wiley, New York, 1984, 3rd Ed.
2. I. M. Ward, *Structure and Properties of Oriented Polymers,* Applied Science Publishers Ltd., London, 1975.
3. L. Mandelkern, *Crystallization of Polymers,* McGraw-Hill Book Co., New York, 1964.
4. G. Farrow and I. M. Ward, *Polymer,* **1,** 330 (1960).
5. N. S. Murthy, Y. P. Khanna, and A. J. Signorelli, *Polym. Engi. Sci.,* **36,** 1254 (1994).
6. D. Hyndman and G. F. Origlio, *J. Polym. Sci.,* **39,** 135 (1959).
7. J. Schultz, *Polymer Materials Science,* Prentice-Hall, Inc., Englewood Cliffs, New Jersey, 1974.
8. N. S. Murthy, H. Minor, C. Bednarczyk, and S. Krimm, *Macromolecules,* **26,** 1712 (1993).
9. Y. Fu, B. Annis, A. Boller, Y. Jin, and B. Wunderlich, *J. Polym. Sci. Part B Polym. Phys.,* **32,** 2289 (1994).
10. A. D. English, *Macromolecules,* **17,** 2182 (1984).
11. D. L. Tzou, P. Desai, A. S. Abhiraman, and T.-H. Huang, *J. Polym. Sci. Part B Polym. Phys. Ed.,* **29,** 49 (1991).
12. K. J. Yoon, P. Desai, and A. S. Abhiraman, *J. Polym. Sci. Part B Polym. Phys. Ed.,* **24,** 1665 (1986).
13. J. P. Runt, *Encyclopedia of Polymer Science and Engineering,* Wiley, New York, 1986, Vol. 4.
14. H. de Vries, *Colloid Polym. Sci.,* **257,** 226 (1979).
15. J. H. Dumbleton, *J. Polym. Sci. Part A-2,* **6,** 795 (1968).
16. M. G. Northolt and H. A. Stuut, *J. Polym. Sci. Polym. Phys. Ed.,* **16,** 939 (1978).
17. Quantachrome Corp., *Multipycnometer Operating Manual, Model MVP-1,* Boynton Beach, Florida (1989).
18. F. J. Balta-Calleja, *X-Ray Scattering of Synthetic Polymers,* Elsevier, Asterdam, 1989.
19. A. Miyake, *J. Polym. Sci.,* **38,** 479 (1959).
20. S. Lin and J. L. Koenig, *J. Polym. Sci., Polym. Phys. Ed.,* **20,** 2277 (1982).
21. J. L. Koenig and D. Kormos, *Contemp. Topics Polym. Sci.,* **3,** 127 (1979).
22. A. E. Tonelli, *Polym. Lett. Ed.,* **11,** 441 (1973).
23. J. R. Havens and D. L. VanderHart, *Macromolecules,* **18,** 1663 (1985).
24. W. Gabriëlse, H. A. Gaur, F. C. Feyen, and W. S. Veeman, *Macromolecules,* **27,** 5811 (1994).
25. H. A. Davis, *J. Textile Inst.,* **82,** 86 (1991).